INSTITUT DE RECERCA EN ENERGIA DE CATALUNYA

Modeling and validation of a flywheel energy storage lab-setup

Francisco Díaz González, PhD
fdiazg@irec.cat

Barcelona, 08.01.2014

Our laboratory...

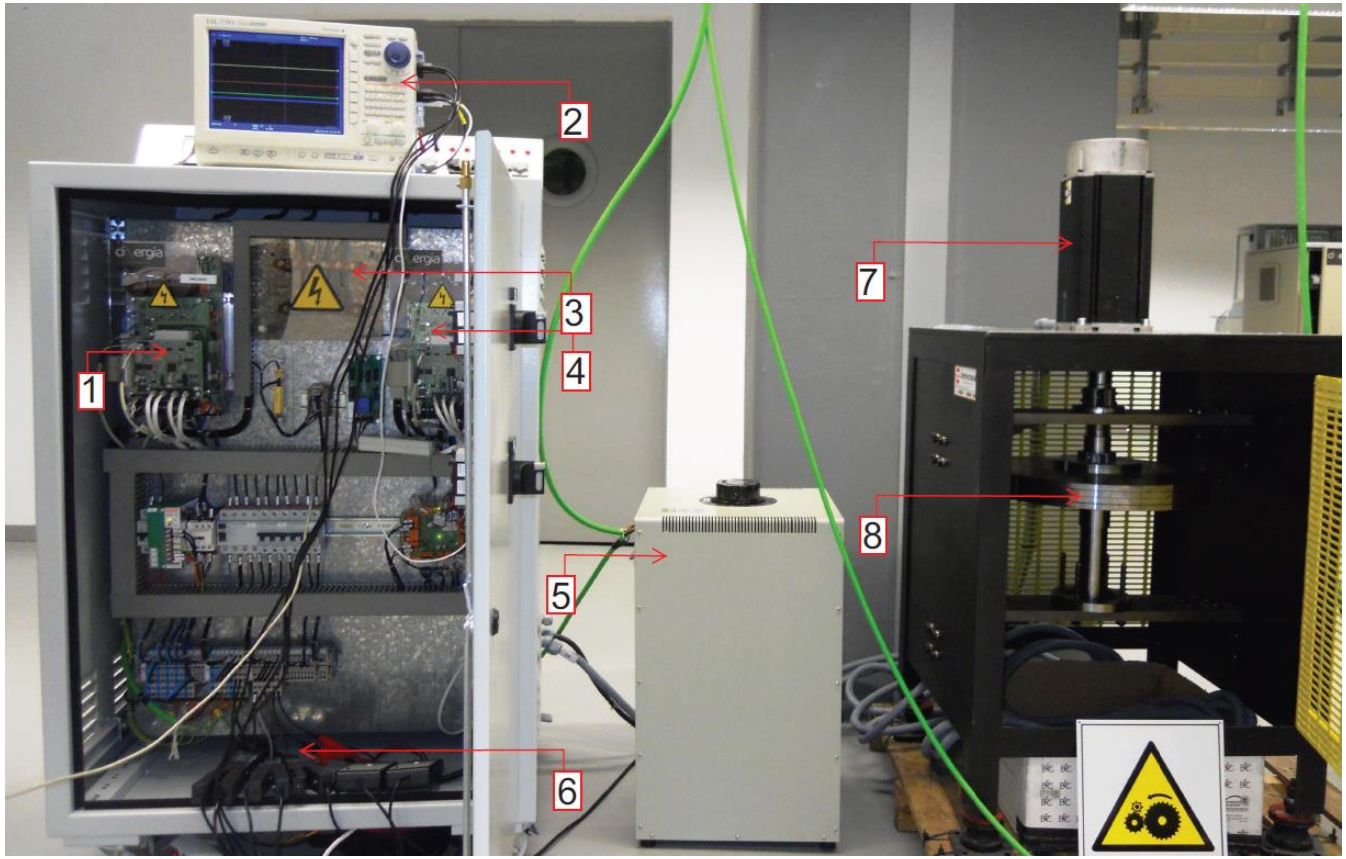

Figure 1: Experimental setup. From left to right: item 1) Grid side converter; item 2) Oscilloscope; item 3) Dc-link; item 4) Machine side converter; item 5) Autotransformer; item 6) Measurement devices; item 7) PMSM; item 8) Rotating disk.

Our laboratory...

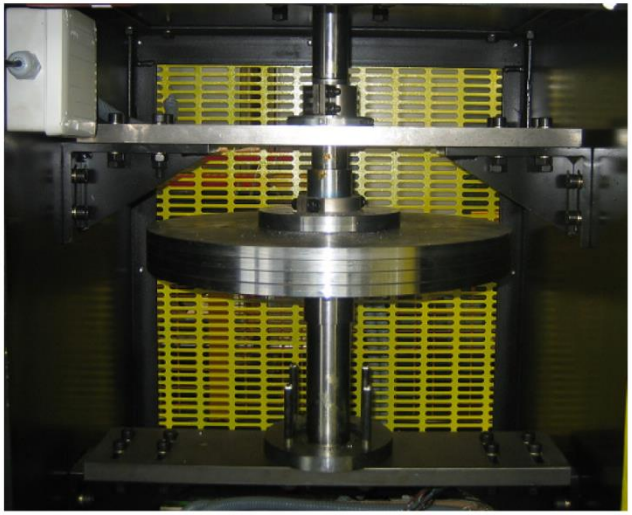

Figure 2: Flywheel rotating disk

...ers and

Our laboratory...

- Header elements
- Emulated devices
- Semi emulated devices
- Real power systems
- Electric vehicle

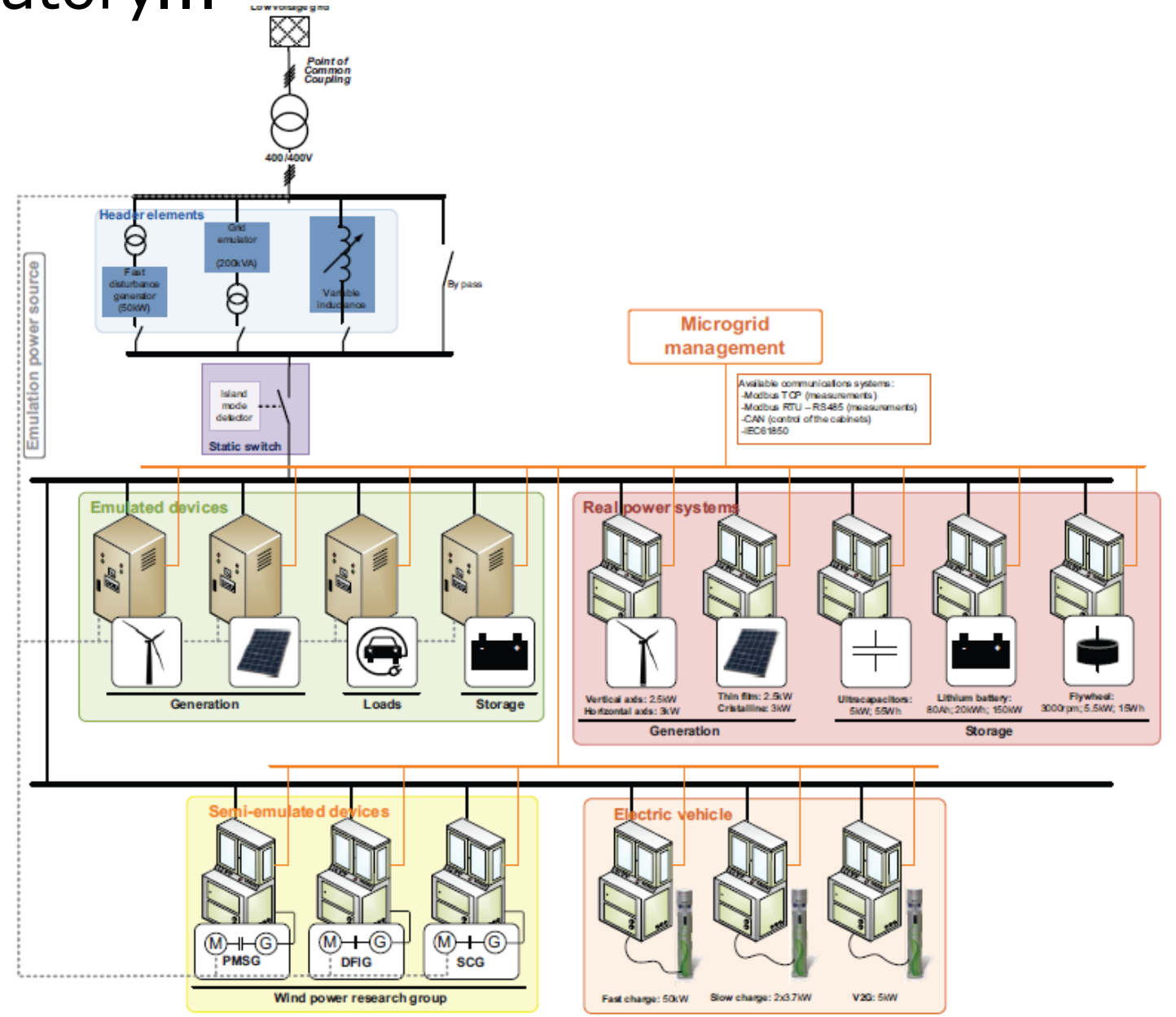

Some literature about Flywheel Energy Storage Systems (FESS) [1-8]

- High efficiency, long cycle life, freedom from depth-of-discharge effects, high power and high energy density, but high self discharge rates

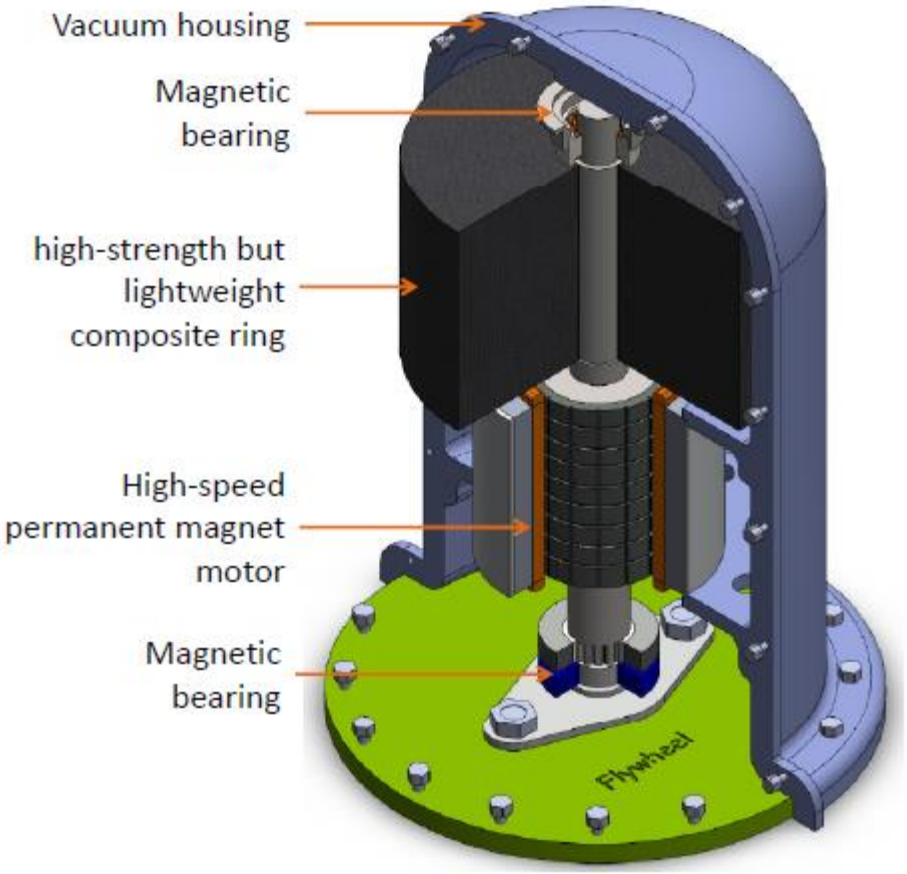

System description

Some examples

Piller

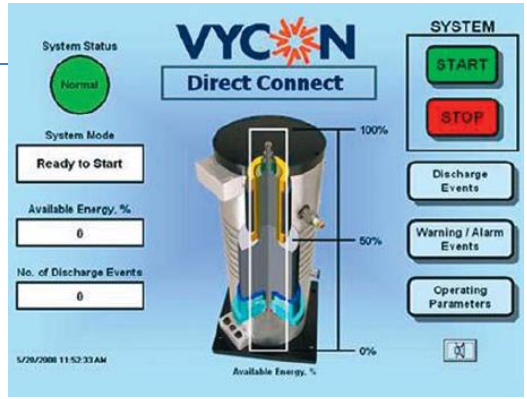

Chloride-Vycon, 215kW
during 5 sec. 61.000 €

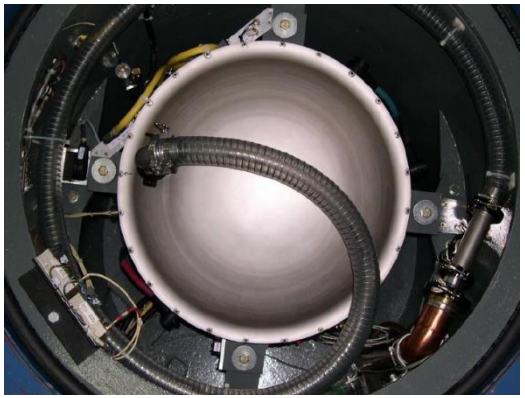

Flywheel energy systems Inc.
100kW, 320Wh 55.000 €

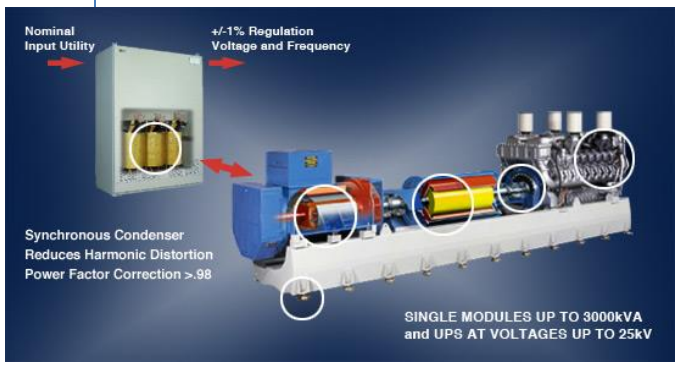

Hitec-ups, 400kW, 230.000€

Pentadyne Clean Energy Storage

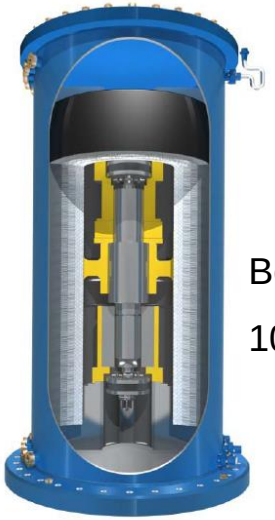

Beacon Power,
100kW, 25kWh

Smart Energy 25 flywheel

System modeling

PMSM and rotating disk modeling

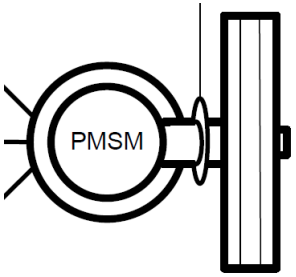

Fig 5. Subsystem modeled

- The system can be modeled as a single mass system,
- The energy losses due to the friction in the bearings have to be taken into account.
- Machine equations in a synchronous *qd0* reference with the electrical frequency of the machine,

$$u_{sq} = R_s i_{sq} + L_q \frac{d}{dt} i_{sq} + \omega_r L_d i_{sd} + \omega_r \psi_{PM}$$

$$u_{sd} = R_s i_{sd} + L_d \frac{d}{dt} i_{sd} - \omega_r L_q i_{sq}$$

← Voltage equations

$$u_{0s} = R_s i_{0s} + L_{ls} \frac{d}{dt} i_{s0}$$

$$T_e = \left(\frac{3}{2}\right)\left(\frac{p}{2}\right)\psi_{PM} i_{sq}$$

← Torque equation

$$\frac{d\omega_r}{dt} = \frac{p}{2}\frac{T_e - T_l}{J}$$

← Equation of motion

System modeling

Power converters modeling

The FESS power converters are in a back-to-back configuration. These electronic power converters are modeled as six force-commutated IGBT power switches connected in a bridge configuration.

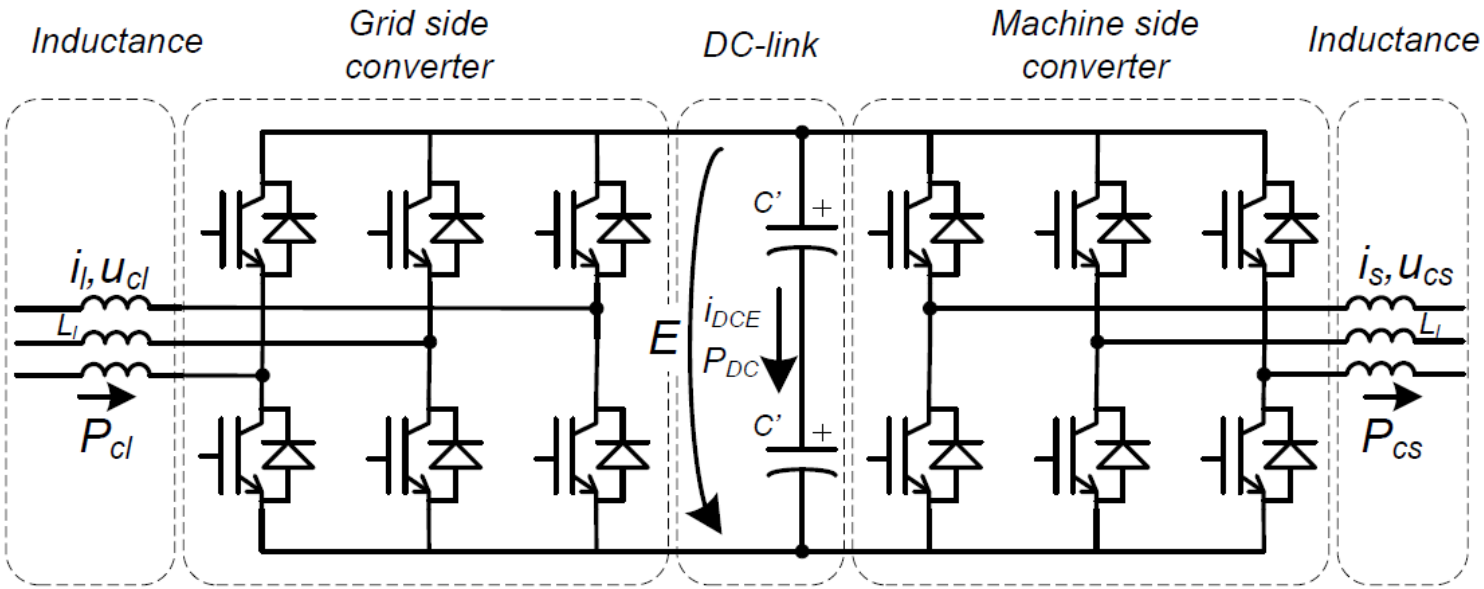

Fig 6. Subsystem modeled

Control system design

The grid side converter controller is responsible for regulating the dc-link voltage and the reactive power exchanged with the external grid. The machine side converter controller regulates the speed and the reactive currents flowing from the electrical motor

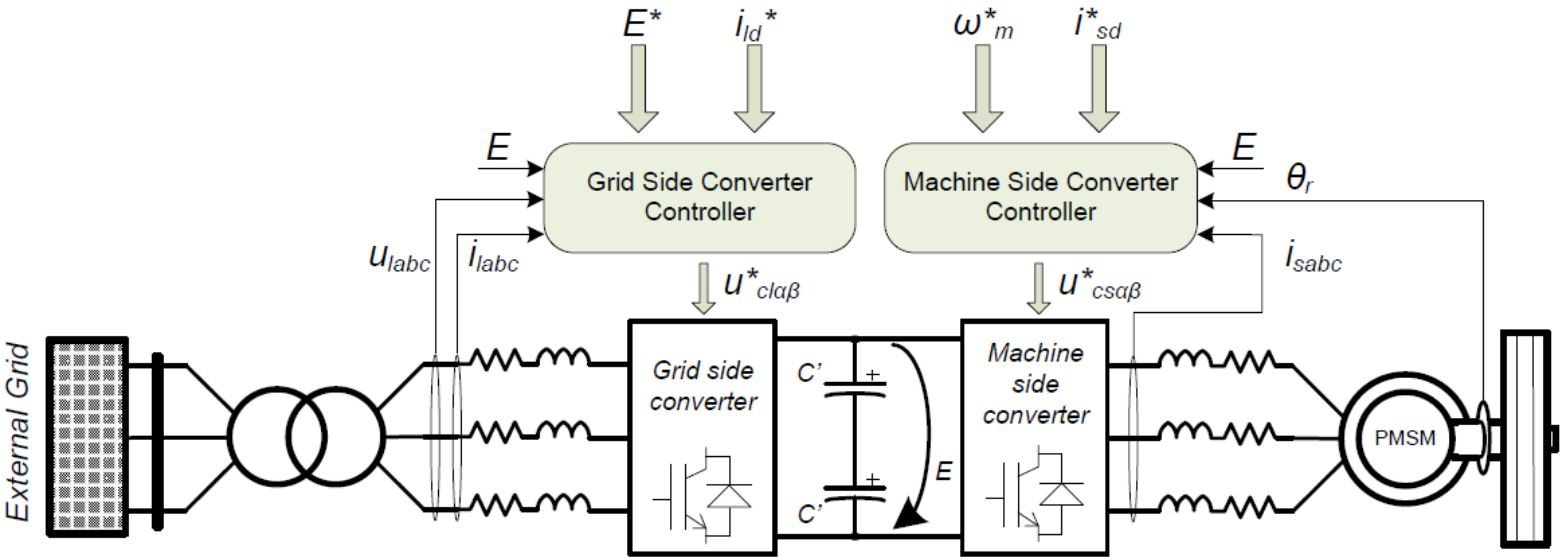

Fig 9. Energy storage system

Control system design

Machine side converter controller

- The machine side converter controller is based on the field oriented vector control algorithm of the PM machine [9-11].
- Its main objective is to control the speed of the servomotor
- Additionally, and thanks to vector control techniques, it is possible to control the reactive current flowing from the stator of the machine by means of regulating the direct-axis stator current i_{sd}.

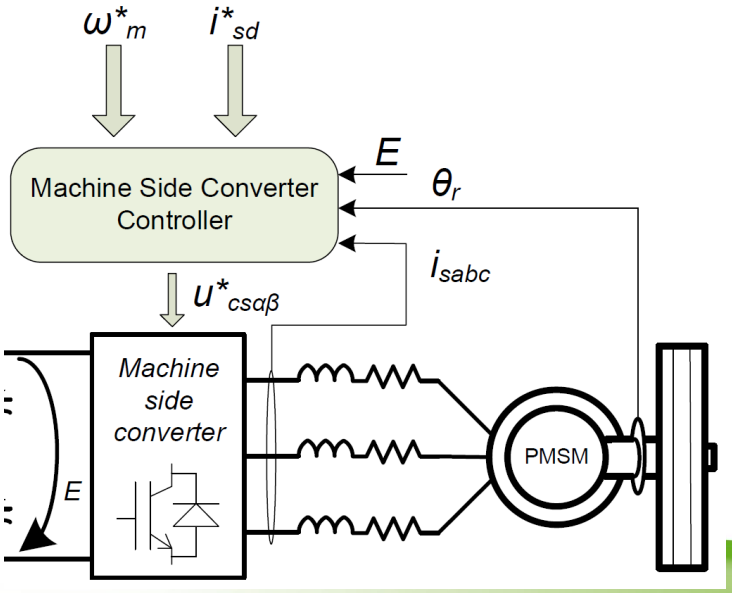

Fig 10. Machine side converter controller

Control system design

Grid side converter controller

The grid side converter controller is responsible for maintaining the DC bus voltage to a constant referenced value. In addition, this controller is in charge of regulating the injected or absorbed reactive power to or from the external grid [12-15]

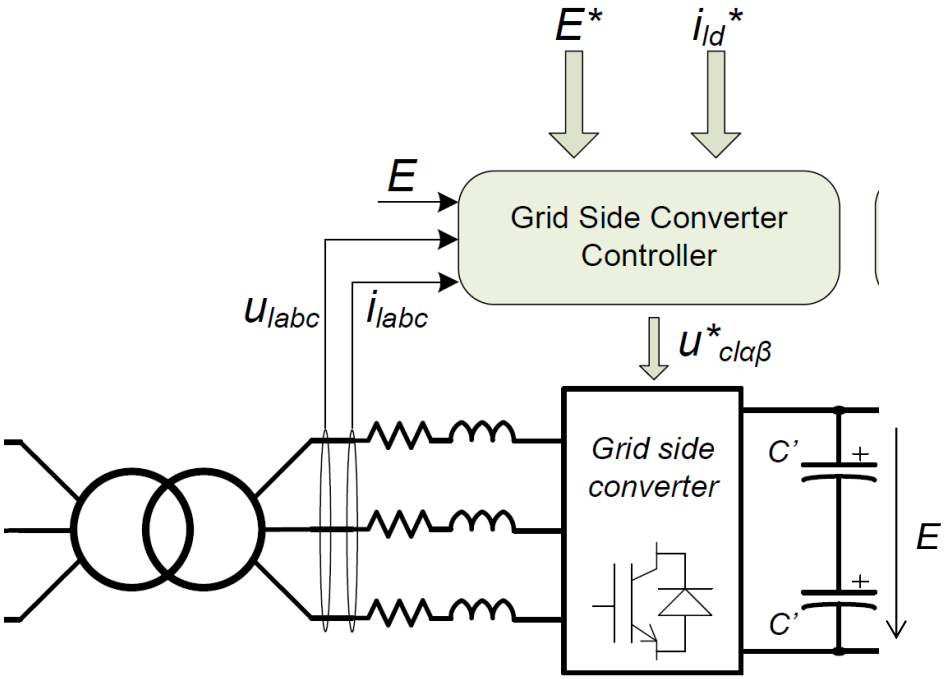

Fig 12. Grid side converter controller

Control system design

Grid side converter controller

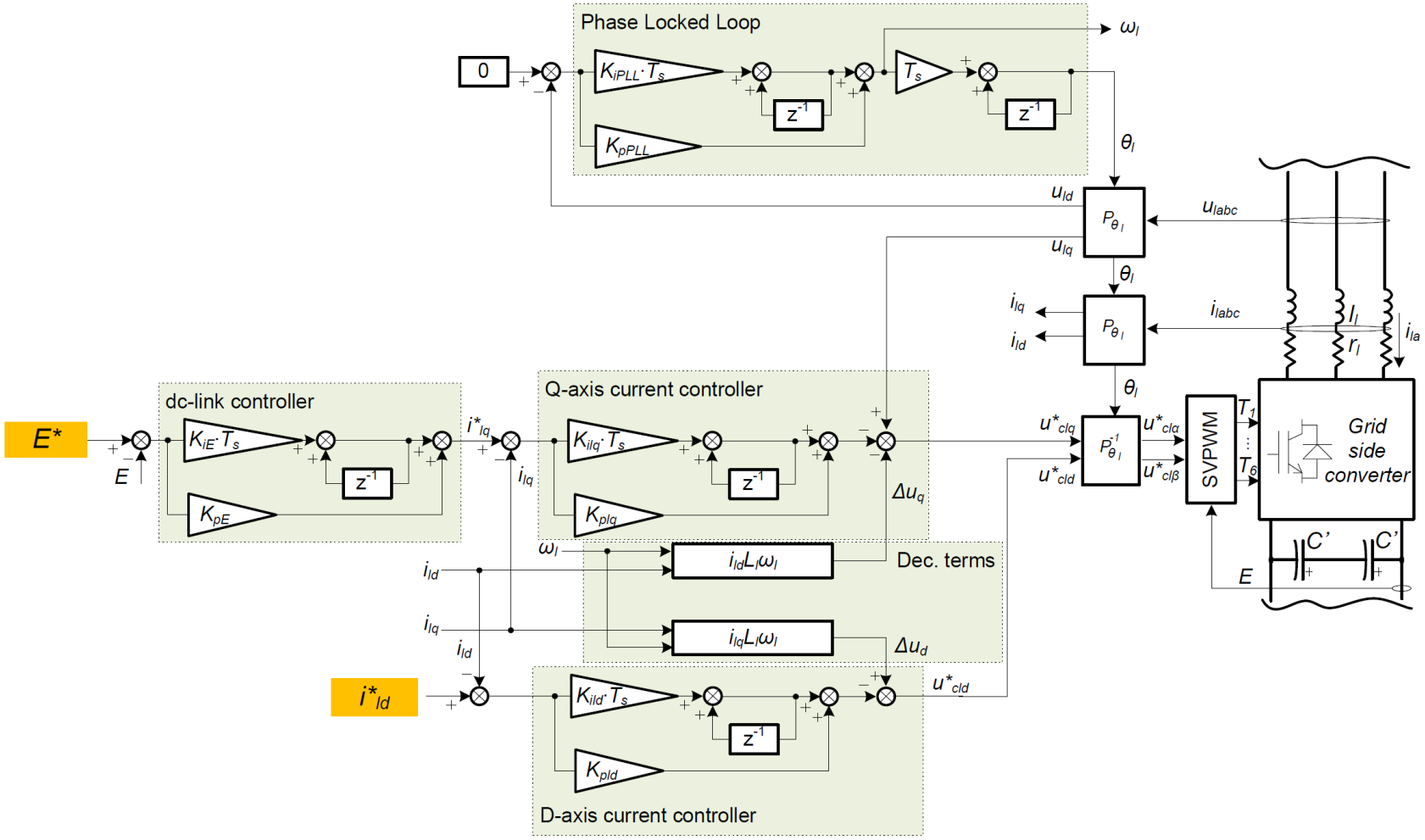

Control system design

Machine side converter controller

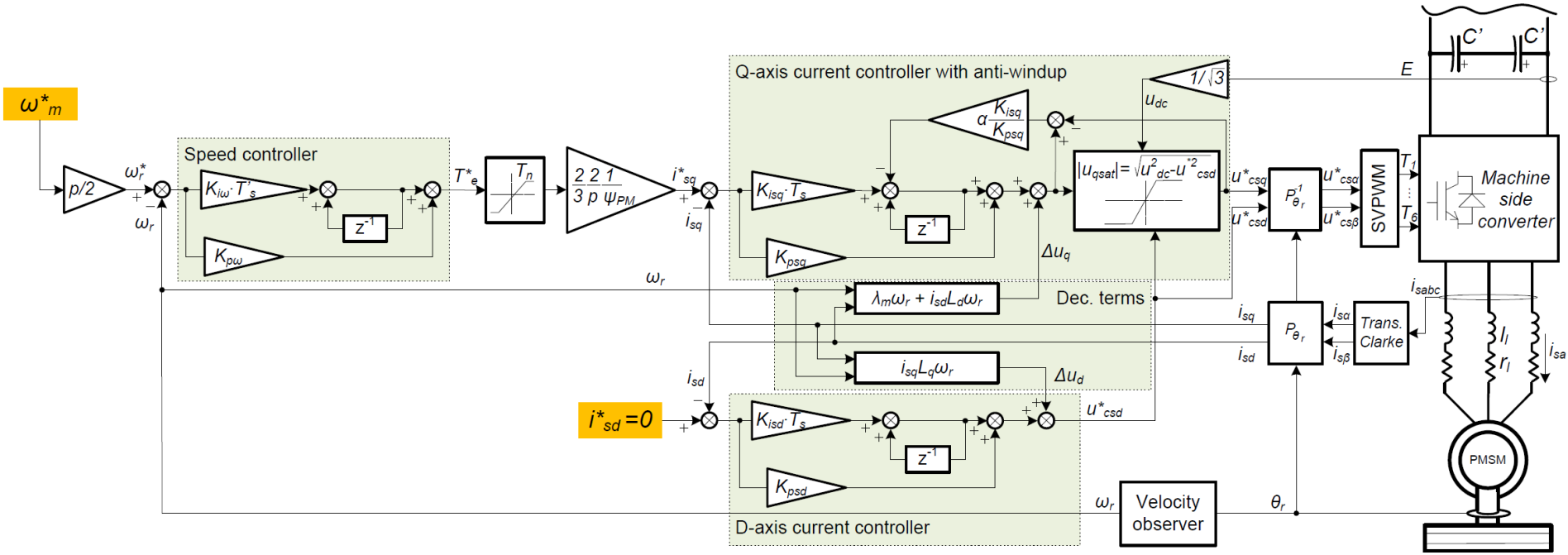

Testing of the experimental setup and model validation

Torque losses of the system

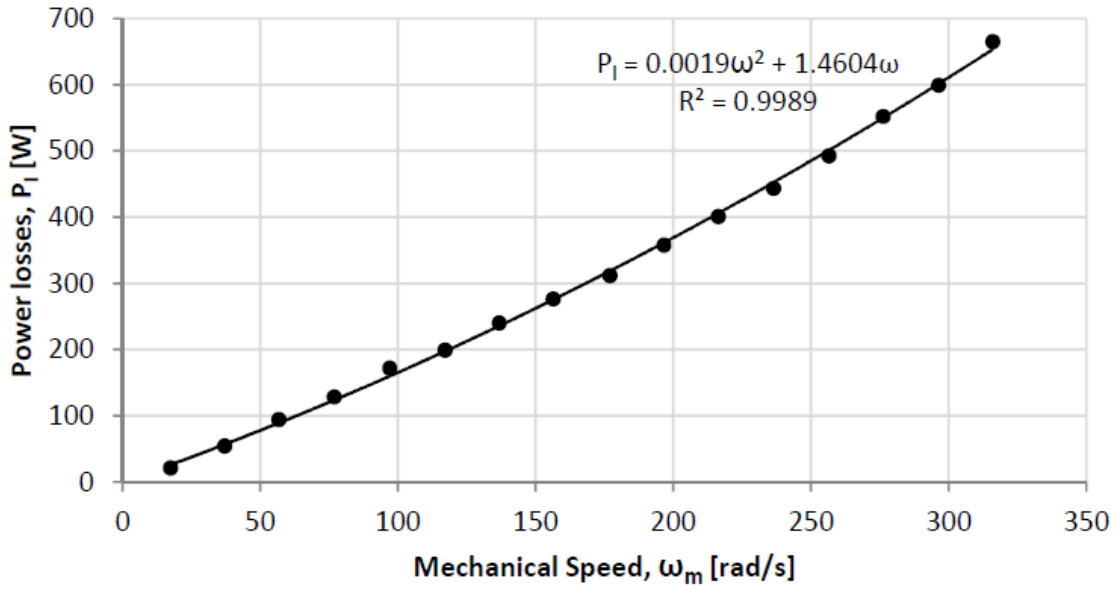

$$T_l = \frac{P_l}{\omega_m} = 0.0019\omega_m + 1.4606$$

Fig 14. Power losses vs mechanical speed

Testing of the experimental setup and model validation

Machine side converter controller testing and validation

DSP sample time: *12 kHz*
Grid voltage: *305 V*
DC link voltage: *650 V*

Table 2: Machine side converter controller parameters

Controller	Proportional gain		Integral gain	
	Symbol	Value	Symbol	Value
Q-axis current controller	K_{psq}	5.74	K_{isq}	567.57
D-axis current controller	K_{psd}	5.74	K_{isd}	567.57
Speed regulator	$K_{p\omega}$	0.193	$K_{i\omega}$	-

Testing of the experimental setup and model validation

Machine side converter controller testing and validation

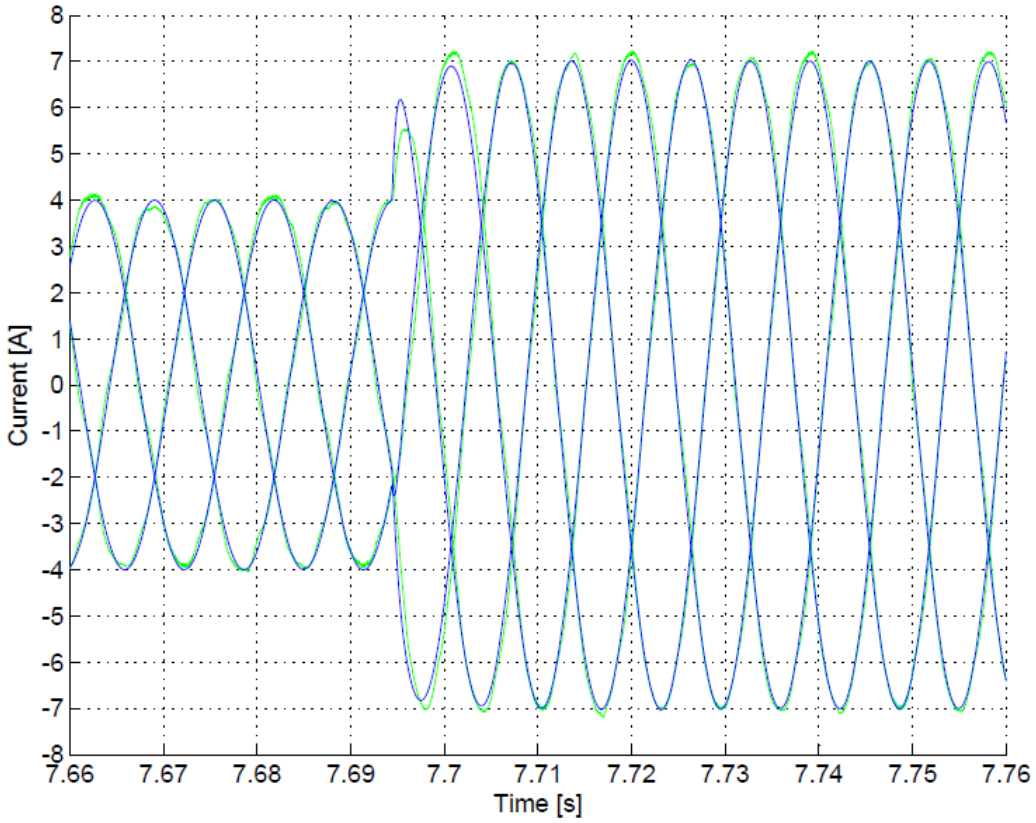

Fig 15. Temporal response to a step-profiled q-axis current reference from 4 to 7 A. Green lines plot measured values while blue lines plot simulation results

Testing of the experimental setup and model validation

Machine side converter controller testing and validation

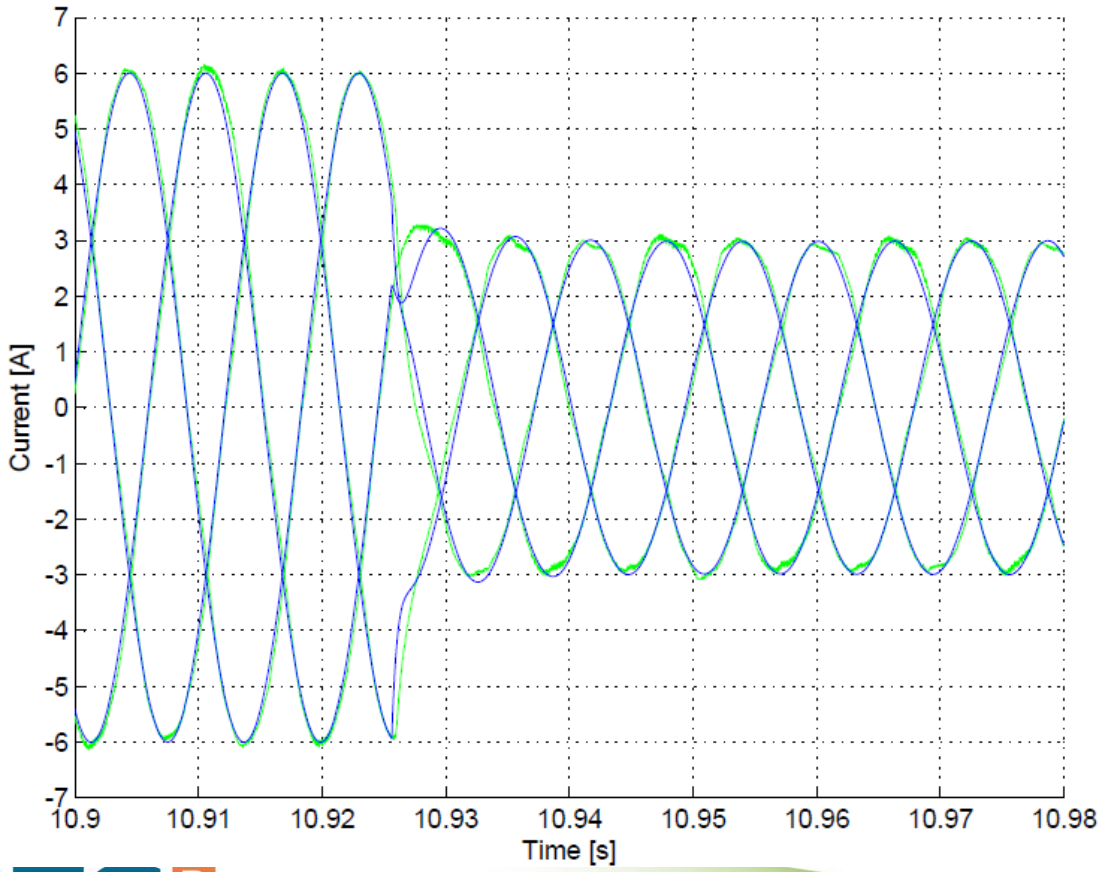

Fig 16. Temporal response to a step-profiled d-axis current reference from 6 to 3 A. Green lines plot measured values while blue lines plot simulation results

Testing of the experimental setup and model validation

Machine side converter controller testing and validation

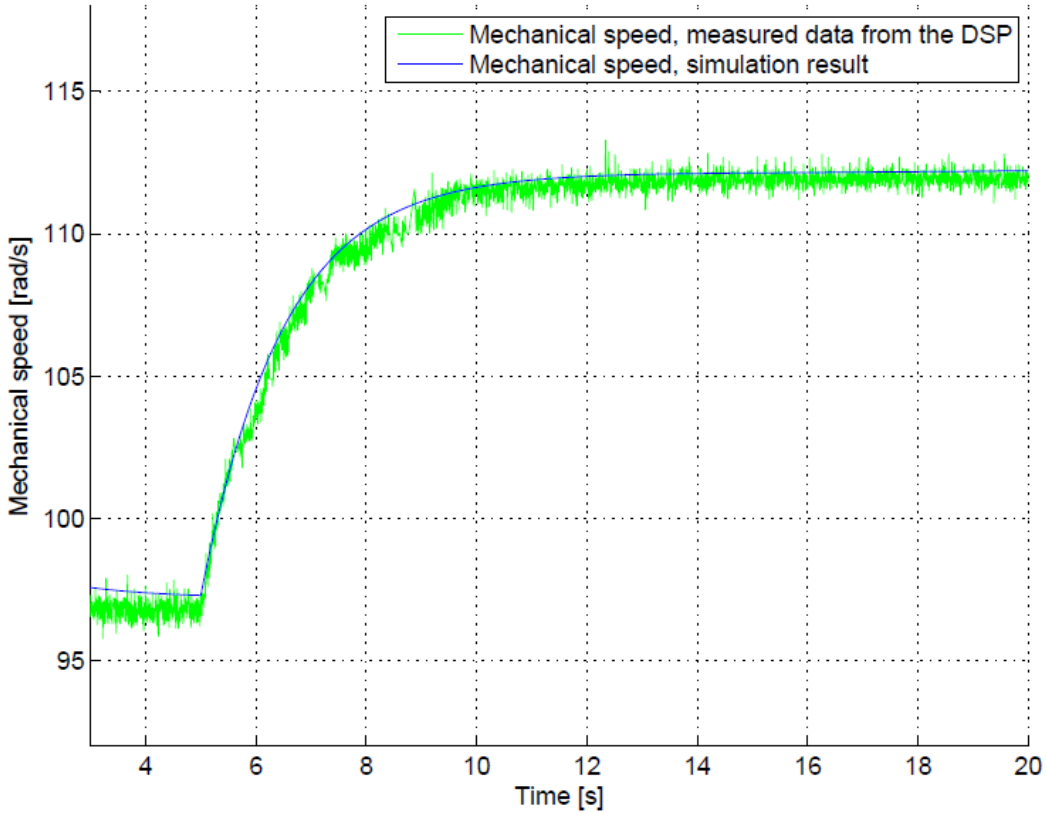

Fig 17. Temporal response to a step-profiled speed reference from 100 rad/s to 115 rad/s. Green lines plot measured values while blue lines plot simulation results

Testing of the experimental setup and model validation

Grid side converter controller testing and validation

DSP sample time: *24 kHz*
Grid voltage: *305 V*
DC link voltage: *650 V*

Table 3: Grid side converter controller parameters

Controller	Proportional gain		Integral gain	
	Symbol	Value	Symbol	Value
Q-axis current controller	K_{plq}	23.51	K_{ilq}	1533.1
D-axis current controller	K_{pld}	23.51	K_{ild}	1533.1
Dc-voltage regulator	K_{pE}	0.1929	K_{pE}	1.113

Testing of the experimental setup and model validation

Grid side converter controller testing and validation

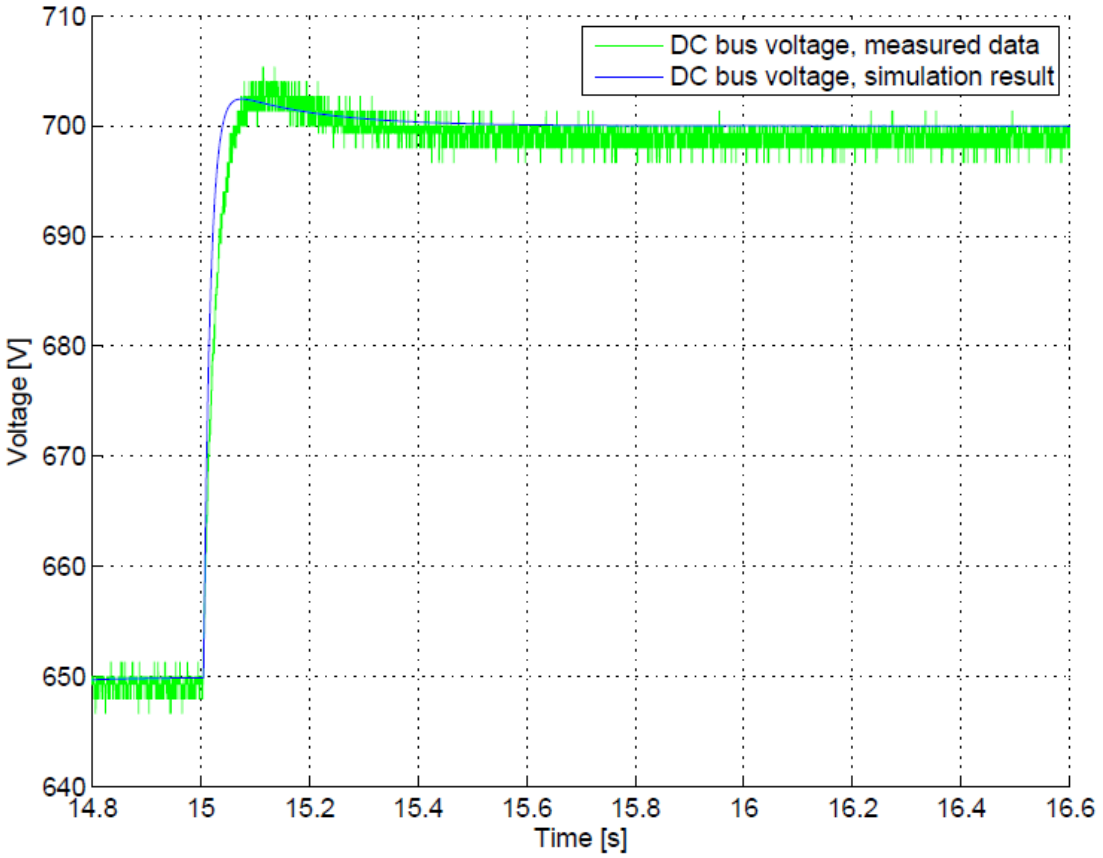

Fig 18. Temporal response to a step-profiled voltage reference from E* equals 650 V to 700 V. Green lines plot measured values while blue lines plot simulation results

Characterization of the energy storage system

Experimental results

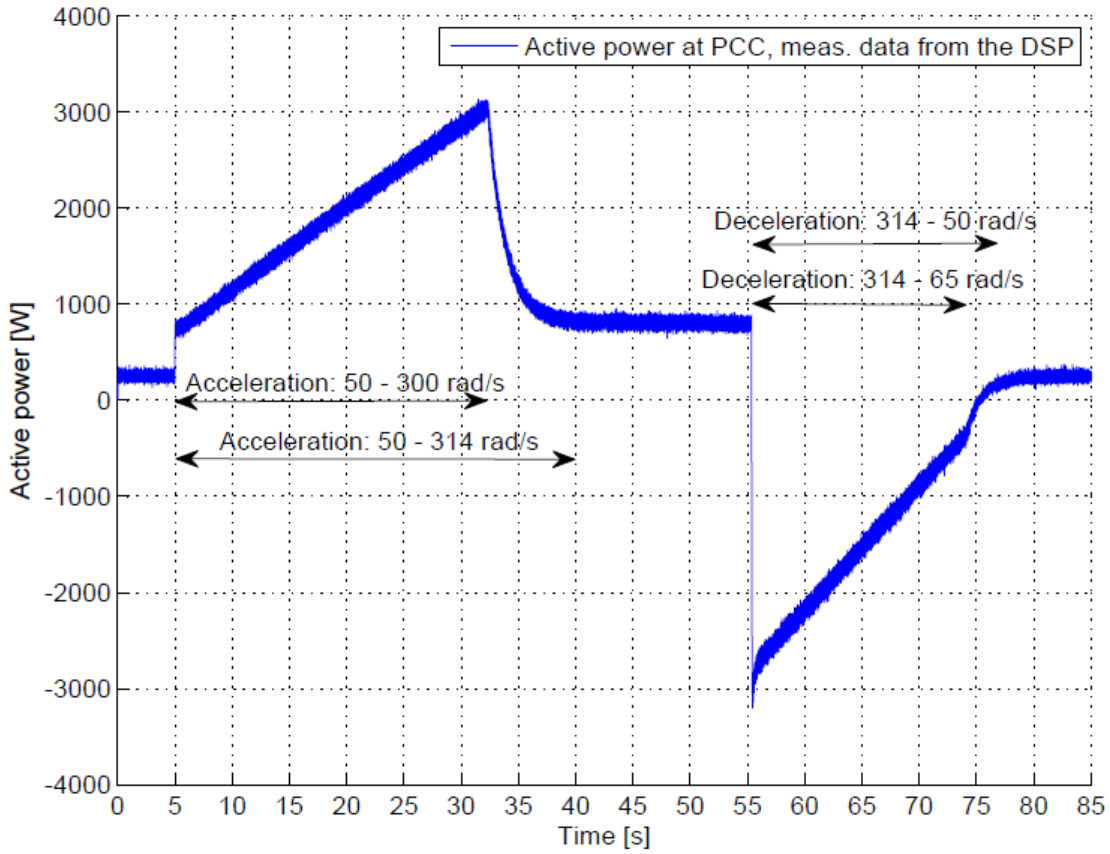

Fig 20. Active power at PCC during an acceleration from 50 rad/s to 314 rad/s and a following deceleration to 50 rad/s

Characterization of the energy storage system

Experimental results

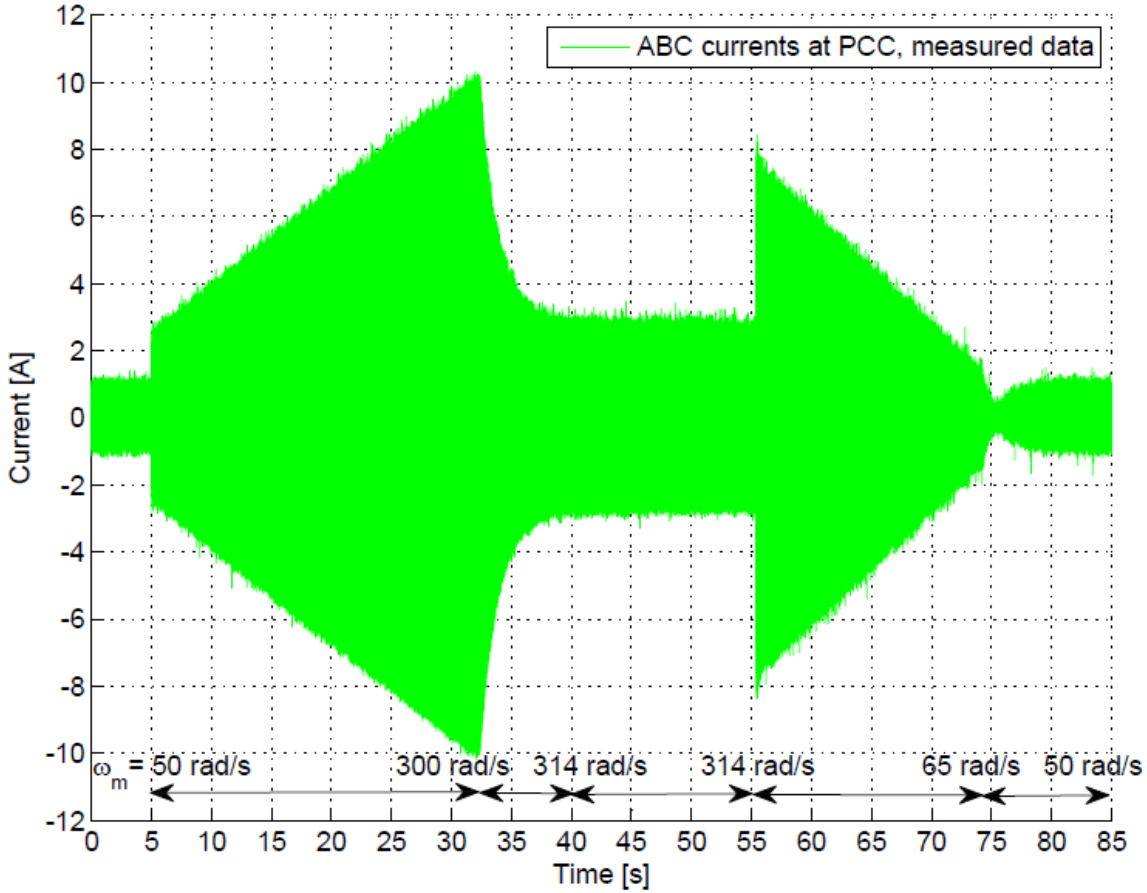

Fig 21. Alternating currents at PCC during an acceleration from 50 rad/s to 314 rad/s and a following deceleration to 50 rad/s

Characterization of the energy storage system

Characteristics

According to IEEE Std 1679-2010, which is a recommended practice for the characterization and evaluation of energy storage technologies in stationary applications [16]:

- The energy rating E_{rating} of the system at a constant stator currents discharge rate of -9 A, while the mechanical speed decreases from 314 rad/s to 65 rad/s is,

$$E_{rating} = \int_{t=55.4s}^{t=74.4s} P(t) \cdot \mathrm{dt} \approx 30\,\mathrm{kW} \cdot \mathrm{s}$$

Characterization of the energy storage system

Characteristics

- The energy eciency during the discharge process is computed as,

$$E_{eff} = \frac{E_{rating}}{E_{k|_{\omega_m=314\text{rad/s}}} - E_{k|_{\omega_m=65\text{rad/s}}}} \cdot 100 = 73\%$$

Conclusions

- In this work, the modeling, control and experimental validation of a flywheel-based energy storage device have been presented.
- A field oriented vector control algorithm has been implemented for governing the servomotor while the instantaneous power theory-based algorithm has been used to manage the active and reactive currents flowing from the grid side converter.
- The modeling, which has been carried out in software Matlab Simulink, and control system design have been validated executing several experiments. Moreover, other characteristics like the torque losses of the system have been determined experimentally.
- The energy capacity of the system has been determined to be 30 kWs. The energy efficiency has been quantified to 73%. Moreover, the power capacity of the system has been limited to 3 kW in order to operate the system within secure operating limits of the power converters.
- Setting up this system opens the door to explore potential applications of flywheel systems in different fields such as microgrids and wind power generation.

References

[1] Beaudin, M., Zareipour, H., Schellenberglabe, A. and Rosehart,W., ”Energy storage for mitigating the variability of renewable electricity sources: An updated review”, Energy for Sustainable Development, 2010, Vol. 14, 302-13

[2] Bolund, B., Bernho, H. and Leijon, M., ”Flywheel energy and power storage systems”, Renewable and Sustainable Energy Reviews, 2007, Vol. 11, 235-258

[3] Jiancheng Zhang, ”Research on Flywheel Energy Storage System Using in Power Network”, International Conference on Power Electronics and Drives Systems, 2005

[4] Jiancheng, Z., Lipei, H., Zhiye, C. and Su, W., ”Research on flywheel energy storage system for power quality”, Proceedings of PowerCon 2002, International Conference on Power System Technology, 2002

[5] Goswami, D. Y., ”Energy conversion”, CRC Press Taylor & Francis Group, 2008

[6] Dai, X., Deng, Z., Liu, G., Tang, X., Zhang, F. and Deng, Z., ”Review on advanced flywheel energy storage system with large scale”, Transactions of China Electrotechnical Society, 2011, Vol. 26, 133-140

[7] Hadjipaschalis, I., Poullikkas, A. and Efthimiou, V., ”Overview of current and future energy storage technologies for electric power applications”, Renewable and Sustainable Energy Reviews, 2009, Vol. 13, 1513-1522

[8] Díaz-González, F., Sumper, A., Gomis-Bellmunt, O. and Villafáfila-Robles, R., ”A review of energy storage technologies for wind power applications”, Renewable and Sustainable Energy Reviews, 2012, Vol. 16, 1356-1371

[9] Krause, P. C.,Wasynczuk, O. and Sudho, S. D., ”Analysis of electric machinery and drive systems”, Wiley, 2002

[10] Terorde, G., ”Electrical drives and control techniques”, Acco, 2004

[11] Arrouf, M. and Bouguechal, N., ”Vector control of an induction motor fed by a photovoltaic generator”, Applied Energy, 2003, Vol. 74, 159-167

[12] Akagi, H., Watanabe, E. H. and Aredes, M., ”Instantaneous power theory and applications to power conditioning”, Wiley Inter-Science, 2007

[13] Domínguez-García, J.L., Gomis-Bellmunt, O., Trilla-Romero, L. and Junyent-Ferré, A., ”Indirect vector control of a squirrel cage induction generator wind turbine”, Computers & Mathematics with Applications, 2012, article in press

[14] Gomis-Bellmunt, O., Junyent-Ferré, A., Sumper, A. and Bergas-Jane, J., ”Permanent magnet synchronous generator oshore wind farms connected to a single power converter”, IEEE Power and Energy Society General Meeting, 2010, 1-6

[15] Junyent-Ferré, A., Gomis-Bellmunt, O., Sumper, A., Sala, M. and Mata, M. ”Modeling and control of the doubly fed induction generator wind turbine”, Simulation Modeling Practice and Theory, 2010, Vol. 18, 1365-1381

[16] IEEE Power & Energy Society, ”IEEE Recommended practice for the characterization and evaluation of emerging energy storage technologies in stationary applications”, IEEE Std 1679-2010, 2010

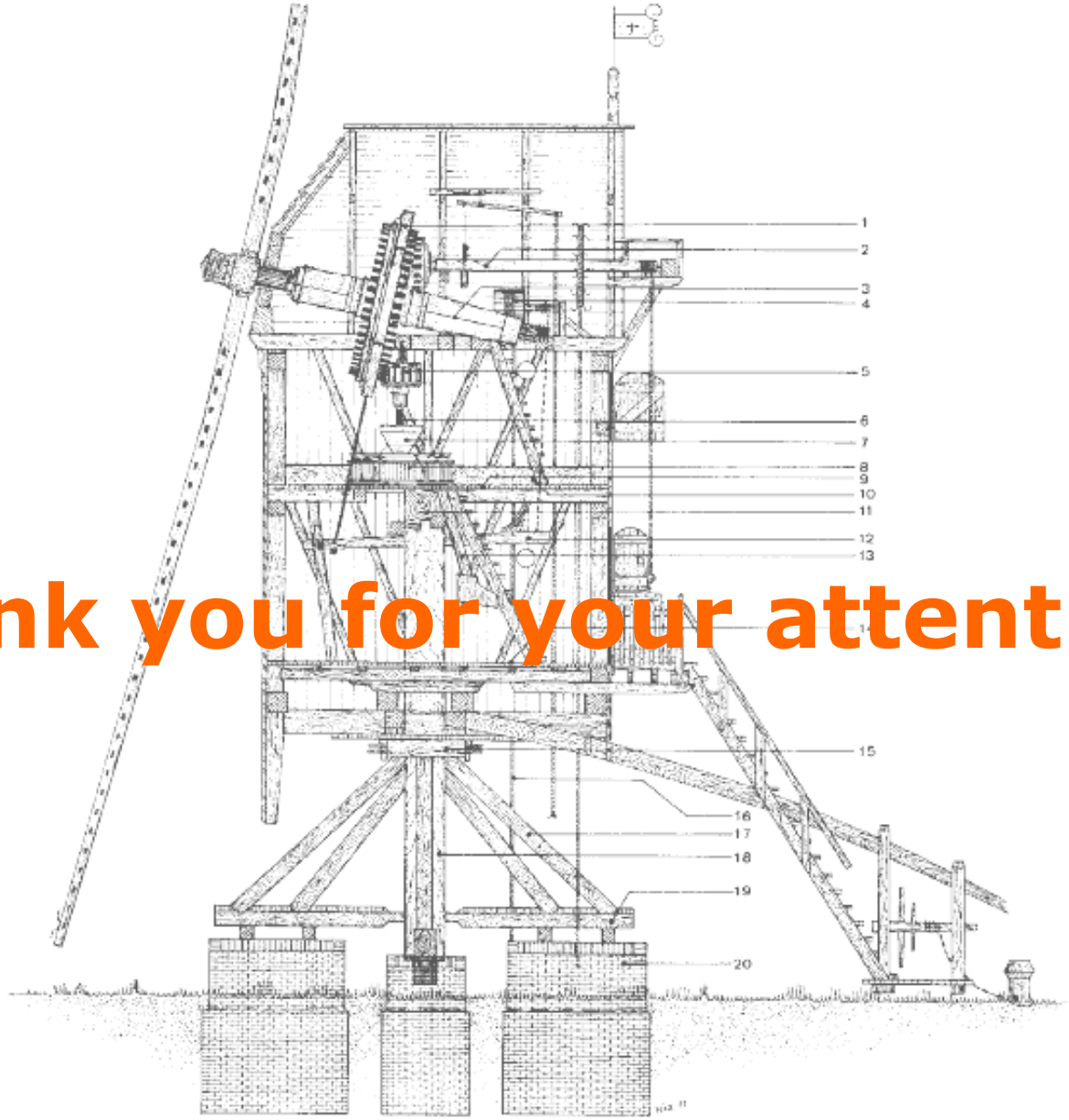

Thank you for your attention